

COMPUTATIONAL STUDIES OF NON-LOCAL ANISOTROPIC  
ALLEN-CAHN EQUATION

MICHAL BENEŠ, Praha, SHIGETOSHI YAZAKI, Miyazaki,  
MASATO KIMURA, Fukuoka

(Received October 15, 2009)

*Abstract.* The paper presents the results of numerical solution of the Allen-Cahn equation with a non-local term. This equation originally mentioned by Rubinstein and Sternberg in 1992 is related to the mean-curvature flow with the constraint of constant volume enclosed by the evolving curve. We study this motion approximately by the mentioned PDE, generalize the problem by including anisotropy and discuss the computational results obtained.

*Keywords:* Allen-Cahn equation, phase transitions, mean-curvature flow, finite-difference method

*MSC 2010:* 35K57, 35K65, 65N40, 53C80

## 1. INTRODUCTION

The paper deals with the initial-boundary value problem for the non-local reaction-diffusion equation

$$(1.1) \quad \begin{aligned} \xi \frac{\partial p}{\partial t} &= \xi \Delta p + \frac{1}{\xi} f_0(p) - \frac{1}{\xi |\Omega|} \int_{\Omega} f_0(p) \, dx, \\ \frac{\partial p}{\partial n} \Big|_{\partial \Omega} &= 0, \quad p|_{t=0} = p_{\text{ini}}, \end{aligned}$$

for the unknown function  $p = p(t, x)$  defined for  $x \in \Omega$  and  $t \in (0, T)$ , where  $\Omega = (0, L_1) \times (0, L_2) \in \mathbb{R}^2$  is a rectangular domain, for simplicity. The parameter  $0 < \xi \ll 1$  is related to the thickness of the interface layer which can develop in parts of the solution with steep gradient. This behaviour is given by the shape of the polynomial

$$f_0(p) = ap(1-p)\left(p - \frac{1}{2}\right),$$

with  $a > 0$  which is derived from a double-well potential  $w_0$  as  $w'_0 = -f_0$ , and is justified by the matched asymptotic expansion. Consequently, the values 0 and 1 of the function  $p$  prevail in  $\Omega$  whereas the transition between them forms a thin interface layer. This allows to understand  $p$  as an indicator of the liquid and solid phases. The function  $p_{\text{ini}}$  is the initial condition.

The problem (1.1) has been introduced in [1] as a modification of the Allen-Cahn equation [2], [3] approximating the mean-curvature flow [7]. In [6] the axisymmetric case was studied to provide information on the singular-limit behaviour of the selected level set. As described e.g. in [8] the problem (1.1) is closely related to the diffuse-interface models of phase transitions. In particular, the non-local character of the equation is connected to the recrystallization phenomena where a fixed previously melted volume of the liquid phase solidifies again. Respecting the fact that a real material always exhibits an anisotropy of the surface energy, this article suggests to modify (1.1) by introducing anisotropy in the relative geometry similarly to [7] and to study numerical solution providing the motion of a selected level set.

## 2. EQUATIONS

As mentioned above, the problem (1.1) is modified using the following framework (compare with [7] and references therein). We consider a nonnegative function  $\Phi: \mathbb{R}^n \rightarrow \mathbb{R}_0^+$  which is smooth, strictly convex,  $\mathcal{C}^2(\mathbb{R}^n \setminus \{0\})$  and satisfies:

$$(2.1) \quad \begin{aligned} \Phi(t\eta) &= |t|\Phi(\eta), \quad t \in \mathbb{R}, \eta \in \mathbb{R}^n, \\ \lambda|\eta| &\leq \Phi(\eta) \leq \Lambda|\eta|, \end{aligned}$$

where  $\lambda, \Lambda > 0$ . The function given by

$$\Phi^0(\eta^*) = \sup\{\eta^* \cdot \eta \mid \Phi(\eta) \leq 1\}$$

is its dual. They satisfy the relations

$$(2.2) \quad \begin{aligned} \Phi_\eta^0(t\eta^*) &= \frac{t}{|t|}\Phi_\eta^0(\eta^*), \quad \Phi_{\eta\eta}^0(t\eta^*) = \frac{1}{|t|}\Phi_{\eta\eta}^0(\eta^*), \quad t \in \mathbb{R} \setminus \{0\}, \\ \Phi(\eta) &= \Phi_\eta(\eta) \cdot \eta, \quad \Phi^0(\eta^*) = \Phi_\eta^0(\eta^*) \cdot \eta^*, \quad \eta, \eta^* \in \mathbb{R}^n, \end{aligned}$$

where the index  $\eta$  means derivative with respect to  $\eta$  ( $\Phi_\eta$  is the total derivative consisting of partial derivatives with respect to components of the vector  $\eta$ ).

The mapping  $\Phi$  plays the role of a distance (norm) replacing the Euclidean distance in the analysis of the problem to be derived from (1.1). Consequently, the dual

mapping  $\Phi^0$  enters the problem (1.1) itself. For this purpose, we define the map  $T^0: \mathbb{R}^n \rightarrow \mathbb{R}^n$  as

$$\begin{aligned} T^0(\eta^*) &= \Phi^0(\eta^*)\Phi_\eta^0(\eta^*) \quad \text{for } \eta^* \neq 0, \\ T^0(0) &= 0. \end{aligned}$$

This allows to define the  $\Phi$ -gradient of a smooth function  $u$ :

$$(2.3) \quad \nabla_\Phi u = T^0(\nabla u) = \Phi^0(\nabla u)\Phi_\eta^0(\nabla u).$$

If we assume that the hypersurface  $\Gamma(t)$  is given by a level set of the field function  $P = P(t, x)$ , then

$$\Gamma(t) = \{\mathbf{x} \in \mathbb{R}^n \mid P(t, x) = \text{const.}\},$$

and the  $\Phi$ -normal vector (the Cahn-Hoffmann vector) and the velocity of  $\Gamma(t)$  given by the field  $P$  are

$$\mathbf{n}_{\Gamma, \Phi} = -\frac{\nabla_\Phi P}{\Phi^0(\nabla P)} = -\frac{T^0(\nabla P)}{\Phi^0(\nabla P)}, \quad v_{\Gamma, \Phi} = \frac{\partial_t P}{\Phi^0(\nabla P)}.$$

The anisotropic curvature is given by the formula

$$\kappa_{\Gamma, \Phi} = \text{div}(\mathbf{n}_{\Gamma, \Phi}).$$

Note that in the isotropic case,  $\Phi(\cdot) = |\cdot|$  and the normal vector, the normal velocity and the isotropic curvature are denoted by  $\mathbf{n}_\Gamma$ ,  $v_\Gamma$  and  $\kappa_\Gamma$ .

*Example.* In practice, the choice of anisotropy is given by the shape of  $\Phi^0$ . In 2D, we typically use the dual metric set as

$$\Phi^0(\eta^*) = \varrho\Psi(\theta),$$

where  $[\varrho, \theta]$  are polar coordinates of  $\eta^*$ . Using the duality relationship  $(\Phi^0)^0 = \Phi$ , we find that

$$\Phi(\eta) = |\eta| \frac{\cos(\theta^* - \theta_0)}{\Psi(\theta^*)},$$

where  $\eta$  has the polar coordinates  $|\eta|$ ,  $\theta_0$ , and  $\theta^*$  is the solution of the equation

$$\tan(\theta^* - \theta_0) = -\frac{\Psi'(\theta^*)}{\Psi(\theta^*)}.$$

Our choice can be  $\Psi(\theta) = 1 + A \sin(m\theta)$ , where  $A \geq 0$  is the anisotropy strength, and  $m = 2, 4, \dots$  the order of symmetry. The convexity condition reads  $A \leq (m^2 - 1)^{-1}$ . In higher dimensions, the anisotropy can explore e.g. various norms of the  $l_p$  type.

**Remark.** The (strong) monotonicity of the operator  $T^0$  is equivalent to the (strict) convexity of the functional

$$\int_{\Omega} \Phi^0(\nabla p)^2 dx.$$

Wulff shape representing the unit ball under the metric  $\Phi$  is defined in [7], and can be parametrized as follows:

$$\begin{aligned} \mathcal{W}: x(\theta) &= \Psi(\theta) \cos(\theta) - \Psi'(\theta) \sin(\theta), \\ y(\theta) &= \Psi(\theta) \sin(\theta) + \Psi'(\theta) \cos(\theta). \end{aligned}$$

In Figure 1, we show examples of various anisotropies in terms of the Wulff shape.

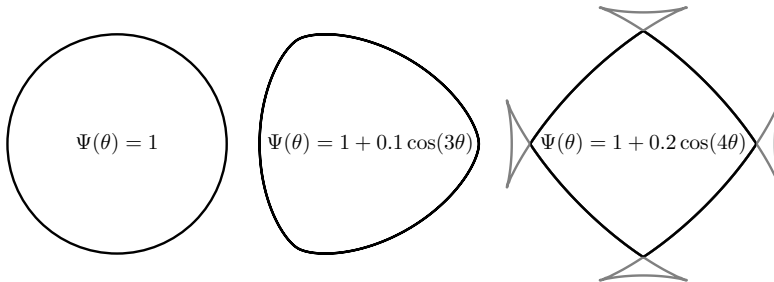


Figure 1. Examples of the Wulff shape as the boundary of the convex interior for presented patterns.

**IBVP.** In analogy to the isotropic problem (1.1), we propose to use the modified Allen-Cahn equation approximating the motion of the manifold  $\Gamma$  through the level set  $\frac{1}{2}$  of its solution (see e.g. [7]). For the sake of simplicity, we are restricted to two-dimensional rectangular domain and homogeneous Neumann boundary conditions.

We choose a rectangular domain  $\Omega = (0, L_1) \times (0, L_2) \subset \mathbb{R}^2$ ,  $x = [x_1, x_2] \in \Omega$ , and the time variable  $t \in (0, T)$ . The problem for the unknown function  $p = p(t, x)$  reads

$$(2.4) \quad \begin{aligned} \xi \frac{\partial p}{\partial t} &= \xi \nabla \cdot T^0(\nabla p) + \frac{1}{\xi} f_0(p) - \frac{1}{\xi |\Omega|} \int_{\Omega} f_0(p) dx, \quad \text{in } (0, T) \times \Omega, \\ \frac{\partial p}{\partial n} \Big|_{\partial \Omega} &= 0 \quad \text{on } (0, T) \times \partial \Omega, \quad p|_{t=0} = p_{\text{ini}} \quad \text{in } \overline{\Omega}. \end{aligned}$$

### 3. NUMERICAL SOLUTION

For the numerical solution of the problem (2.4), we use the method of lines combined with the finite-difference method on a uniform spatial grid with  $N_1, N_2$  denoting the number of mesh points in the direction of  $x_1, x_2$ , respectively. We also introduce the following notation:

$$\begin{aligned} h_1 &= \frac{L_1}{N_1}, \quad h_2 = \frac{L_2}{N_2}, \\ \omega_h &= \{[ih_1, jh_2] \mid i = 1, \dots, N_1 - 1; j = 1, \dots, N_2 - 1\}, \\ \bar{\omega}_h &= \{[ih_1, jh_2] \mid i = 0, \dots, N_1; j = 0, \dots, N_2\}, \\ \gamma_h &= \bar{\omega}_h \setminus \omega_h, \\ u_{\bar{x}_1, ij} &= \frac{u_{ij} - u_{i-1, j}}{h_1}, \quad u_{x_1, ij} = \frac{u_{i+1, j} - u_{ij}}{h_1}, \quad \bar{\nabla}_h u = [u_{\bar{x}_1}, u_{\bar{x}_2}], \\ u_{\bar{x}_2, ij} &= \frac{u_{ij} - u_{i, j-1}}{h_2}, \quad u_{x_2, ij} = \frac{u_{i, j+1} - u_{ij}}{h_2}, \quad \nabla_h u = [u_{x_1}, u_{x_2}], \\ (u, v)_h &= \sum_{i, j=1}^{N_1, N_2} h_1 h_2 u_{ij} v_{ij} \end{aligned}$$

for  $u, v: \bar{\omega}_h \rightarrow \mathbb{R}$ . The set of grid functions defined on  $\bar{\omega}_h$ , respecting the discrete Neumann boundary conditions ( $b_c(p^h)|_{\gamma_h} = 0$ ), and endowed with the scalar product  $(\cdot, \cdot)_h$  is denoted by  $\mathcal{H}_h$ .

On  $\omega_h$ , the semi-discrete scheme has the form

$$(3.1) \quad \begin{aligned} \xi^2 \frac{dp^h}{dt} &= \xi^2 \nabla_h \cdot T^0(\bar{\nabla}_h p^h) + f_0(p^h) - \frac{1}{|\Omega|_h} (f_0(p^h), 1)_h, \\ b_c(p^h)|_{\gamma_h} &= 0, \quad p^h(0) = \mathcal{P}_h p_{\text{ini}}, \end{aligned}$$

where its solution is a map  $p^h: \langle 0, T \rangle \rightarrow \mathcal{H}_h$ ,  $\mathcal{P}_h: \mathcal{C}(\bar{\Omega}) \rightarrow \mathcal{H}_h$  is a restriction operator,  $|\Omega|_h = (N_1 - 1)(N_2 - 1)h_1 h_2$ . The resulting system of ordinary differential equations in time is solved by the Runge-Kutta-Merson scheme as in [8].

**Remark.** It can be observed that the scheme satisfies the mass constraint  $(p^h(t), 1)_h = (p^h(0), 1)_h$ .

#### 4. COMPUTATIONAL STUDIES

We use the scheme (3.1) to perform a series of computational studies showing the behavior of the solution to (2.4) itself as well as the behavior of the level set  $\frac{1}{2}$  of the solution which is shown (see [6]) to be close to the constrained mean-curvature flow

$$v_\Gamma = -\kappa_\Gamma + \frac{1}{|\Gamma|} \int_\Gamma \kappa_\Gamma \, dl,$$

and close to the mean-curvature flow under some circumstances:

$$v_\Gamma = -\kappa_\Gamma.$$

We try to extend this experience to the anisotropic setting of these two laws

$$(4.1) \quad v_{\Gamma, \Phi} = -\kappa_{\Gamma, \Phi} + \frac{1}{|\Gamma|_\Phi} \int_\Gamma \kappa_{\Gamma, \Phi} \, dl,$$

$$(4.2) \quad v_{\Gamma, \Phi} = -\kappa_{\Gamma, \Phi},$$

where

$$|\Gamma| = \int_\Gamma dl, \quad \text{and} \quad |\Gamma|_\Phi = \int_\Gamma \Phi^0(\mathbf{n}_\Gamma) \, dl.$$

The computations are analyzed using the following measured quantities:

- Area enclosed by  $\Gamma$  (it should be approximately constant)  $A = \int_{\text{Int}\Gamma} dx$ .
- Curve energy (anisotropic length)  $|\Gamma|_\Phi = \int_\Gamma \Phi^0(\mathbf{n}_\Gamma) \, dl$ .
- Anisoperimetric ratio (it should approach the value 1)  $\text{Aniso} = |\Gamma|_\Phi^2 / (4A|W|)$ , where  $|W|$  is the Wulff-shape area.
- Mass (it must be constant due to (3.1))  $M(t) = (p^h(t), 1)_h$ .

The following examples demonstrate how the solution of (2.4) approaches the conserved law (4.1) where the curve pattern converges to the Wulff shape given by the crystalline anisotropy, or the usual law (4.2) where the curve vanishes.

**Example 1.** The first study shows the behavior of the solution when the initial condition mimics a four-folded curve given by the formula  $r_0(s) = 1 + 0.3 \cos(4s)$ ,  $s \in \langle 0, 2\pi \rangle$ . The motion on the time interval  $\langle 0, 0.4 \rangle$  driven by the anisotropic problem (2.4) leads to the formation of the corresponding steady curve adopting the Wulff shape. The anisotropy is given by the formula

$$\Psi(\theta) = 1 + 0.025 \cos(6\theta),$$

and the limiting law at large time scales is approaching (4.1). The interface thickness is  $\xi = 0.035$ , and the numerical mesh size  $h_1 = h_2 = 0.03$ . The CPU time of the

computation was 145.45 s on Pentium IV, 1.66 MHz. From Table 1, the time evolution of the enclosed area, curve energy, anisoperimetric ratio and mass can be seen. The slide-down of values of  $A$  agrees with [1]—in short time, the evolution law for the curve differs from the long-term evolution law.

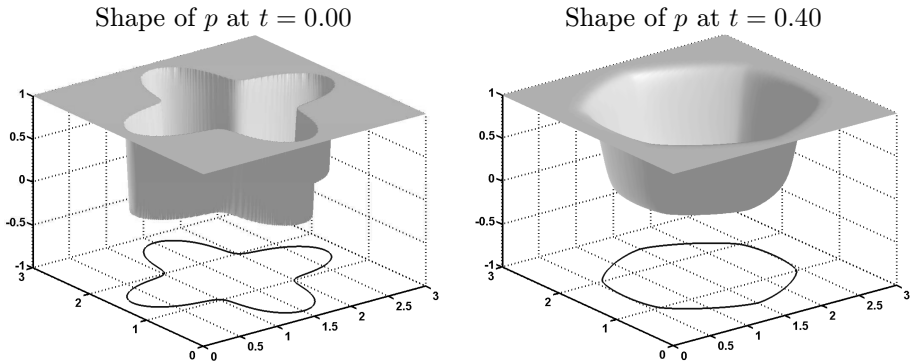


Figure 2. Solution of the Allen-Cahn equation with projection of the level set  $p = \frac{1}{2}$  for Example 1.

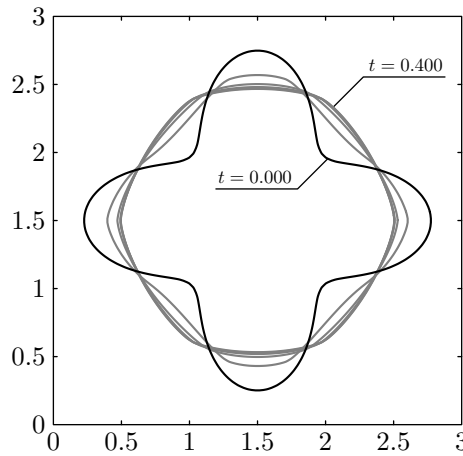


Figure 3. Dynamics of the level set for Example 1.

Time	enclosed area	curve energy	anisoperimetric ratio	mass
0.00	3.2829324353	8.1675881993	1.6349034454	5.5350801809
0.08	3.1997527356	6.5855428285	1.0905187217	5.5350801809
0.16	3.1999598410	6.3353602567	1.0091703716	5.5350801809
0.24	3.1989548827	6.3097806184	1.0013520526	5.5350801809
0.32	3.1973191899	6.3071531255	1.0010301162	5.5350801809
0.40	3.1982783461	6.3065026391	1.0005235003	5.5350801809

Table 1. Measured data for Example 1.

Example 2. The second study shows the behavior of the solution when the initial condition mimics two four-folded curves one inside the other, given by the formulas  $r_0(s) = 1 + 0.2 \cos(4s)$  and  $r_1(s) = 0.5 + 0.2 \cos(4s)$ ,  $s \in \langle 0, 2\pi \rangle$ . The anisotropy is given by the formula

$$\Psi(\theta) = 1 + 0.3 \cos(4\theta).$$

In agreement with [6] the motion on the time interval  $\langle 0, 0.4 \rangle$  driven by the anisotropic problem (2.4) leads to the fast shrinking of the internal curve according to the mean-curvature flow (4.2) and to the evolution of the external curve towards the corresponding steady curve adopting the Wulff shape by (4.1). The interface thickness is  $\xi = 0.035$ , and the numerical mesh size  $h_1 = h_2 = 0.03$ . The CPU time of the computation was 57.55 s on Pentium IV, 1.66 MHz.

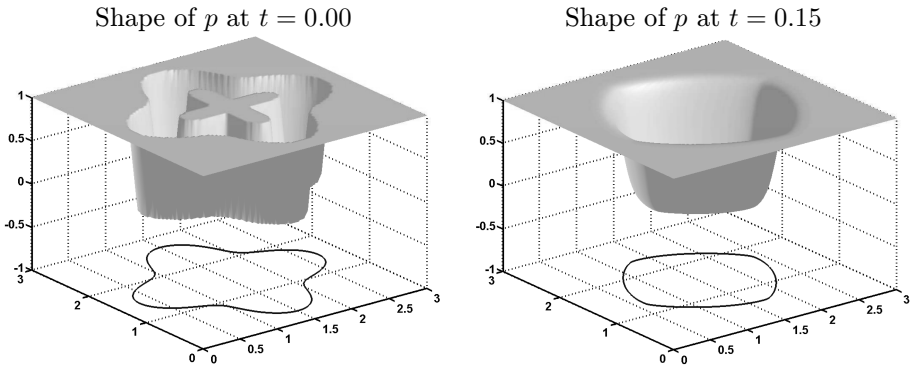


Figure 4. Solution of the Allen-Cahn equation with projection of the outer level set  $p = \frac{1}{2}$  for Example 2.

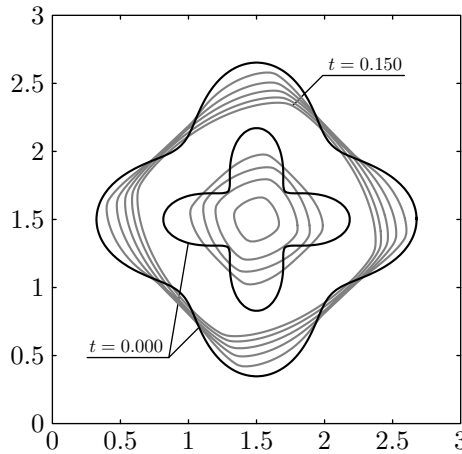


Figure 5. Dynamics of the level set for Example 2.



## 5. CONCLUSION

The paper introduces a numerical scheme allowing to perform computational studies of the anisotropic nonlocal Allen-Cahn equation. The studies confirmed the theoretical indications that the solution approaches the conserved mean-curvature flow in long term. Any additional curve located in the interior moves according to the usual law of motion by mean curvature. This behaviour is in agreement with the recrystallization phenomena in the solid phase.

*Acknowledgement.* The first author was partly supported by the project MSM 6840770010 “Applied Mathematics in Technical and Physical Sciences” of the Ministry of Education, Youth and Sports of the Czech Republic. The second and third authors were partly supported by the project LC06052 “Jindřich Nečas Center for Mathematical Modelling” of the Ministry of Education, Youth and Sports of the Czech Republic.

### *References*

- [1] *J. Rubinstein, P. Sternberg:* Nonlocal reaction-diffusion equation and nucleation. *IMA J. Appl. Math.* *48* (1992), 249–264. zbl
- [2] *S. Allen, J. Cahn:* A microscopic theory for antiphase boundary motion and its application to antiphase domain coarsening. *Acta Metall.* *27* (1979), 1084–1095.
- [3] *J. W. Cahn, J. E. Hilliard:* Free energy of a nonuniform system III. Nucleation of a two-component incompressible fluid. *J. Chem. Phys.* *31* (1959), 688–699.
- [4] *J. E. Taylor, J. W. Cahn:* Linking anisotropic sharp and diffuse surface motion laws via gradient flows. *J. Statist. Phys.* *77* (1994), 183–197. zbl
- [5] *L. Bronsard, R. Kohn:* Motion by mean curvature as the singular limit of Ginzburg-Landau dynamics. *J. Differential Equations* *90* (1991), 211–237. zbl
- [6] *L. Bronsard, B. Stoth:* Volume-preserving mean curvature flow as a limit of a nonlocal Ginzburg-Landau equation. *SIAM J. Math. Anal.* *28* (1997), 769–807. zbl
- [7] *M. Beneš:* Diffuse-interface treatment of the anisotropic mean-curvature flow. *Appl. Math., Praha* *48* (2003), 437–453. zbl
- [8] *M. Beneš:* Mathematical and computational aspects of solidification of pure substances. *Acta Math. Univ. Comenian.* *70* (2001), 123–152. zbl

*Author’s address:* Michal Beneš, Czech Technical University in Prague, Praha, Czech Republic, e-mail: [michal.benes@fjfi.cvut.cz](mailto:michal.benes@fjfi.cvut.cz); Shigetoshi Yazaki, University of Miyazaki, Miyazaki, Japan, e-mail: [yazaki@cc.miyazaki-u.ac.jp](mailto:yazaki@cc.miyazaki-u.ac.jp); Masato Kimura, Kyushu University, Fukuoka, Japan, e-mail: [masato@math.kyushu-u.ac.jp](mailto:masato@math.kyushu-u.ac.jp).